RSC Advances

PAPER

Cite this: *RSC Adv.*, 2020, **10**, 4949

The morphology of poly(terminal vinyl dimethicone-*co*-methyl methacrylate-*co*-*n*-butyl acrylate)/pigment composite film and its application in pigment printing of polyester fabric

Zhijie Chen, *[a] Xudong Hu,[b] Xianghong Wang[a] and Zhong Xiang[b]

Received 26th November 2019
Accepted 20th December 2019

DOI: 10.1039/c9ra09888g

rsc.li/rsc-advances

In this study, a series of poly(terminal vinyl dimethicone-*co*-methyl methacrylate-*co*-*n*-butyl acrylate)/pigment composite particles (P(DMS-Acr)/PB CPs) were successfully prepared *via* miniemulsion polymerization and their latex film microstructures on were examined carefully using transmission electron microscopy (TEM), field emission scanning electron microscopy (FESEM), atomic force microscopy (AFM) and so on. Significant phase separation was observed after film formation, and the copper phthalocyanine blue (PB) particles tend to distribute in the polysiloxane island phase. After baking at 120 °C, the protrusions were generated. With increasing amount of vinyl terminated polydimethylsiloxane (ViPDMS) or baking time, the number of the protrusions became more and the appearance of the protrusions tends to be sharp. When the P(DMS-Acr)/PB CPs were applied in fabric printing, a continuous film was formed on the surface of the fabric at room temperature and therefore the gaps between yarns were blocked. However, the gaps in the fabric reappeared after baking at 120 °C, which could be attributed to the rapid flow of the polymer component. Finally, the fiber was coated with a layer of latex film containing a large number of mastoid structures, and the printed fabric could still retain the majority of the gaps between yarns and between fibers. Therefore, the printed fabric exhibited excellent performances such as good air permeability, softness, and rubbing fastness.

Introduction

Pigment printing has numerous advantages in terms of photosensitivity and transparency, and its process is more eco-friendly as compared with that of traditional dye coloring.[1–4] Commonly, organic pigments attach to the fabric surface in the form of a pigment/polymer blended film.[5–7] However, these pigment particles usually tend to agglomerate with each other in the polymer blend matrix, resulting in poor printing properties. [8–12] Moreover, in order to promote the color rubbing fastness of printed fabric, the surface of the textile was usually covered with a thick layer of continuous polymer film, leading to poor air permeability and softness.

To overcome the above mentioned defects, encapsulation of organic pigment particles by an adhesive polymeric shell was regarded as one of the most effective methods. To date, encapsulation of organic pigment *via* emulsion polymerization, [13–17] miniemulsion polymerization[18–21] and suspension polymerization[22–24] has been reported by many researchers. It was found that the pigment dispersibility in the polymer film was significantly improved after encapsulation. Currently, polyacrylate (PAcr) was widely used for organic pigment encapsulation, due to its superior properties such as good cohesiveness, high gloss and transparency as well as excellent film forming property. Accordingly, thin composite film can be formed on the fabric surface by using PAcr/PB composite particles (CPs) emulsion; meanwhile, the rubbing fastness and hand feel of paint printing fabrics could also be improved.[25,26] However, the resulting PAcr/PB composite film still has several inherent defects, such as poor water resistance and rough feeling; moreover, the yarn gap of fabric would be blocked by the latex film, resulting in reduced air permeability. Polysiloxane was reported to have various special properties, such as wonderful water repellency and weather resistance, low surface free energy, low glass transition temperature, high flexibility, and excellent thermal stability.[27,28] Copolymerization of acrylate monomer with organosilicone monomer can not only enhance the flow ability of the resulting polymer molecular chain, but also reduce surface tension and endow the polymer film with "smooth" feeling.[29–31] Therefore, if the polysiloxane could be incorporated into the composite particles, the polymer component would flow quickly during the film formation process. In other words, the polymer component would tend to

[a]Key Laboratory of Surface Modification of Polymer Materials, Wenzhou Polytechnic, Wenzhou, 325035, China. E-mail: chenzhijie5262@163.com

[b]Key Laboratory of Advanced Textile Materials and Manufacturing Technology, Ministry of Education, Zhejiang Sci-Tech University, Hangzhou, Zhejiang 310018, China

coat every filament and the yarn gap of fabric would not be blocked, thereby increasing the breathability of printed fabric.

There are lots of papers on silicone-modified polyacrylates *via* emulsion polymerization or miniemulsion polymerization. Jiang *et al.* use the hydroxyl-containing poly(dimethyl siloxane) (PDMS-OH) to modified polyacrylate. And nanoscale polyacrylate core–shell latex particles with a modification of core by PDMS-OH were prepared by means of seeded emulsion polymerization and used as novel binders for fabric pigment printing.[32] Huang *et al.* use styrene (St), *tert*-butyl acrylate (tBA) and α-bromoisobutyryl-containing poly(dimethylsiloxane) (PDMS-Br_m) to make a kind of polymeric pigment dispersants *via* atom transfer radical polymerization.[33] These studies provide good possibilities for silicone-modified polyacrylates, but it should be noted that the types of silicones used in these studies are different, and more importantly, these polymerizations are performed in absence of pigment particles. When these composite latexes are used in pigment printing, they must be mixed with pigment particles. So there may also have some problems about dispersibility of pigment in blended film, which described above. There is little information regarding the encapsulation of organic pigment particles by using ViPDMS to modified polymeric shell and its application in printed fabric.

In the present work, in order to improve the application performance of organic pigment capsules and explore the composite film morphology of silicone-modified polyacrylate in the presence of pigment particles the silicone modified polyacrylate in the presence of pigment particles. P(DMS-Acr)/PB composite particles (CPs) were synthesized by one-step miniemulsion polymerization of methyl methacrylate (MMA), butyl acrylate (BA), vinyl polydimethyl siloxane (ViPDMS) in the presence of PB. The microstructure of the CPs films on the surface of aluminum substrate were carefully examined by using various technologies. Subsequently, the synthesized CPs was coated on polyester fabrics, and the evolution of surface morphology and structure on fabrics during baking was investigated in detail. On this basis, a mechanism of film formation on polyester fabric was proposed. Moreover, the hydrophobicity, air permeability, softness and rubbing fastness of the printed fabric were also evaluated.

Experimental

Materials

Copper phthalocyanine blue (PB, C.I. Pigment Blue 15) was obtained from Hangzhou Baihe Chemical Co. Ltd. Vinyl polydimethyl siloxane (ViPDMS, $M_n = 35\,000$, viscosity = 5000 cp) was supplied by Shenzhen Lianhuan Organic Silicon Material Co., LTD. Methyl methacrylate (MMA, Analytical Reagent (AR)), butyl acrylate (BA, AR) were obtained from Kermel Chemical Co. Ltd, Tianjing. Potassium persulfate (KPS, AR), sodium dodecylsulfate (SDS, AR), octylphenol ethoxylate (OP-10) and hexadecane (HD, AR) were purchased from Aladdin Chemistry Co., Ltd. Printing thickener (PTF) were purchased from Guangdong Nanhui New Material Co., Ltd.

Preparation of P(DMS-Acr)/PB CPs

The SDS and OP-10 were mixed with deionized water and stirred at 200 rpm for 10 min (aqueous phase). Meanwhile, ViPDMS, MMA, BA and HD were mixed together (oil phase), and the PB was then uniformly dispersed in the oil phase. The oil and aqueous phases were then mixed by using a mechanical agitator at 500 rpm for 30 min to form a homogeneous emulsion. Thereafter, the resultant emulsion was further homogenized by ultrasonication for 10 min under magnetic agitation in an ice bath. The resultant miniemulsion was introduced into a 500 mL glass jacket reactor, and the reaction system was heated to 70 °C then and purged with nitrogen for 30 min. Subsequently, aqueous KPS solution was injected to start the polymerization and the stirring speed was maintained at 200 rpm. The polymerization reaction lasted for 7 h for a high monomer conversion. The detailed reaction recipes are presented in Table 1.

Preparation of printed fabric

The printed fabric was prepared as follow: in order to increase the consistency, a certain amount of thickener PTF (0.55 g) was added to the synthesized miniemulsion (20 g). Afterward, the miniemulsion was printed on the surface of the polyester plain weave fabric by using a magnet printing machine (Minmdf-767, Zimmer, Austria). The printed fabric was dried at 25 °C, and then baked at 120 °C in a thermostatic oven.

Characterization

Dynamic light scattering (DLS)

Particle sizes and polydispersities (PDIs) of the P(DMS-Acr)/PB CPs were analyzed by DLS (Zetasizer Nanoseries, Malvern) at 25 °C under a scattering angle of 90° at a wavelength of 633 nm. The preparation of the DLS samples was as follows: 0.02 mL the P(DMS-Acr)/PB CPs dispersion was added to 5 g water. Then the aqueous dispersion was treated by sonication at 500 W for 15 min; finally, the aqueous dispersion was transferred to a polystyrene cuvette. Particle sizes were reported as the average of three measurements.

The viscosity of pigments/monomer mixture

The viscosity of MMA, BA, ViPDMS, and PB mixture was measured by DV-II + Pro viscometer of American Bolfield Company. The S2 rotor was selected and the test speed was set

Table 1 Reaction recipes of the miniemulsion polymerization (g)

Run	MMA	BA	ViPDMS	PB	HD	SDS	OP-10	KPS	Water
1	5.0	5.0	0	0.5	0.2	0.3	0.2	0.1	88.7
2	4.0	4.0	2	0	0.2	0.3	0.2	0.1	89.2
3	4.5	4.5	1	0.5	0.2	0.3	0.2	0.1	88.7
4	4.0	4.0	2	0.5	0.2	0.3	0.2	0.1	88.7
5	3.5	3.5	3	0.5	0.2	0.3	0.2	0.1	88.7
6	3	3	4	0.5	0.2	0.3	0.2	0.1	88.7
7	2.5	2.5	5	0.5	0.2	0.3	0.2	0.1	88.7

to 100 rpm. The viscosity were reported as the average of three measurements.

Phase structure of latex film

Phase structure of latex film was observed by transmission electron microscope (TEM, JSM-3010, Japan) with an acceleration voltage of 80 kV. TEM sample was prepared as follows. 3 g of CPs emulsion was introduced into a polytetrafluoroethylene mould. The diameter and depth of container in the mould were 3 cm and 500 μm, respectively. A series of latex films were then prepared after drying at a temperature of 25 °C and a humidity of 50% for 24 h. Subsequently, ultrathin film was prepared by using a frozen sections technology with slicing machine, and then used for TEM characterization.

Surface morphology and microstructure

Surface morphology and microstructure of latex film were observed by using a field emission scanning electron microscopy (FESEM, Hitachi SU8010) with an acceleration voltage of 3 kV. Diluted emulsion was dropped on several clean silicon wafers, and dried at 25 °C. Some of silicon wafers were further baked at 120 °C for 5 min. The surface morphology and microstructure of film before and after baking were then examined. Surface morphology and microstructure of printed fabric were observed by using a tungsten filament scanning electron microscopy (TFSEM, JSM-5610LV) with an acceleration voltage of 3 kV. Surface topography of latex film was examined by using an atom force microscopy (AFM, XE-100E, Park System, Korea). AFM samples were prepared as follows. Diluted emulsion was dropped onto a clean silicon wafer and the thin film was prepared by the spin coating method (5000 rpm for 30 s). Subsequently, the prepared film was baked at 120 °C for a certain time before examination.

Water contact angle measurement

Water contact angle (WCA) measurements were performed on a contact angle goniometer (DSA-20, Kruss, Germany) by the sessile drop method at room temperature. Typically, five water drops were placed on the fabric surface and the average value of contact angles was taken for each sample.

Air permeability and rubbing fastness measurement

Air permeability was measured by Digital Breathalyzer (YG461E, Ningbo Textile Instrument Factory, China). First, the sample was hold on the test round table, making sure that the test points are flat. Secondly, a gasket should be placed on the low-pressure side of the sample to prevent air leakage. Start the suction fan to allow the air to pass through the sample and adjust the flow rate. When the pressure is stable, record the air flow rate.

The dry/wet rubbing colour-fastness of the printed polyester fabric was determined by a rubbing tester (680MD, UK) according to AATCC8-2007 test method.

Phase structure of P(DMS-Acr)/PB film

Fig. 1 shows the particle size distribution of P(DMS-Acr)/PB CPs prepared with addition of different contents of ViPDMS. It was found that the average particle size of P(DMS-Acr)/PB CPs increased from 151 to 199 nm and the PDI value was around 0.3 with the ViPDMS content increasing from 0 to 30%. However, when the ViPDMS content reached 40%, polydisperse CPs were obtained but the size of larger particle size exceeded 490 nm. Furthermore, when the ViPDMS content reached 50%, a serious agglomeration of P(DMS-Acr)/PB CPs would happen, so the particle size is larger than 800 nm and the PDI value is large. This is presumably because the viscosity of the oil phase (monomer mixture) increased significantly with the increase of ViPDMS content (Fig. 2).

The phase structure of P(DMS-Acr)/PB film was observed and the TEM images of representative latex film (run 1, 2, 5) was shown in Fig. 3. For PAcr/PB CPs film, the PB particles were evenly dispersed in the PAcr substrate (Fig. 3a and b), which was consistent with previous report.[34] For P(DMS-Acr) latex film (Fig. 3c and d), polysiloxane phase (island phase) with various size was formed and dispersed in the PAcr substrate, due to the incompatibility of polysiloxane and PAcr.[19] In contrast, the P(DMS-Acr)/PB film exhibited a complex morphology and phase structure. As shown in Fig. 3e and f, almost all of the pigment particles preferred to distribute in polysiloxane phase rather than PAcr phase. The shape of polysiloxane phase containing pigments became irregular as compared with that in P(DMS-Acr) CPs film. In addition, part of polysiloxane phase did not contain any pigment particles, which might be attributed to the asymmetrical encapsulation of pigment during the mini-emulsion copolymerization.[35]

Surface morphology of P(DMS-Acr)/PB film on aluminum substrate

In order to well understand the film formation process on fabric, the film morphology on aluminum substrate was examined at first. Herein, the surface morphology of the P(DMS-Acr)/PB and PAcr/PB films was observed before and after baking, just as shown in the FESEM image of Fig. 4. As shown in Fig. 4a, the surface of P(DMS-Acr)/PB CPs film prepared at 25 °C

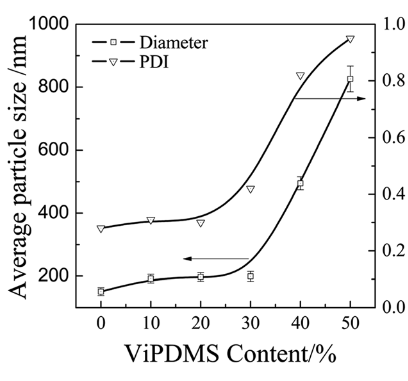

Fig. 1 Particle size of P(DMS-Acr)/PB nanocapsules with different ViPDMS contents.

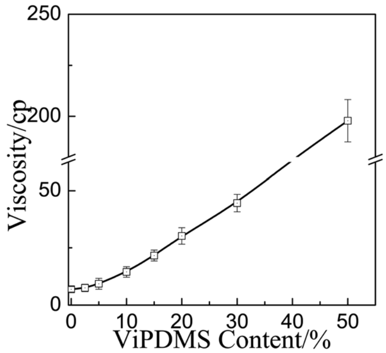

Fig. 2 Viscosity of pigment/monomer dispersion with different ViPDMS content.

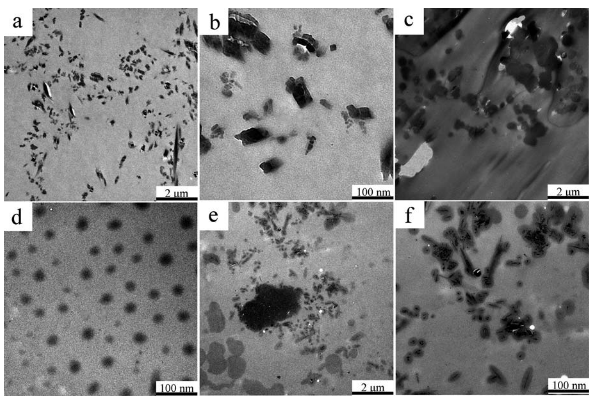

Fig. 3 Typical TEM micrographs of the composite particles film made from the latex of the PAcr/PB (a and b), P(DMS-Acr) (c and d), P(DMS-Acr)/PB (e and f) CPs film using the ultrathin frozen sections.

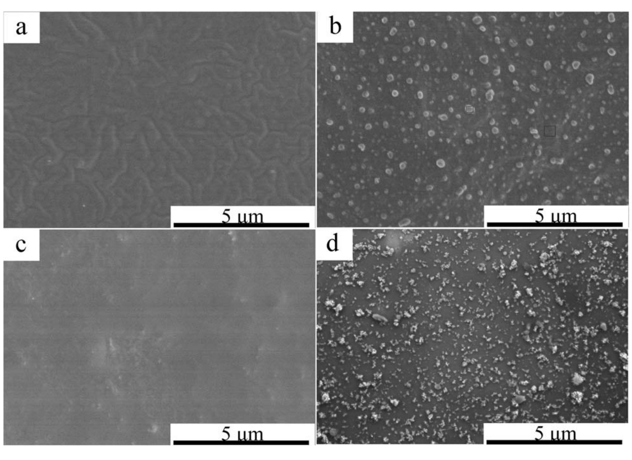

Fig. 4 FESEM images of P(DMS-Acr)/PB (a and b) and PAcr/PB CPs (c and d) film (a and c) before baking, (b and d) after baking 5 min.

was relatively flat. However, after baking for 5 min, the film surface became rough and a lot of protrusions appeared (Fig. 4b). In contrast, no similar protrusion was observed for the PAcr/PB film, but the pigment particles seem to be exposed on the film surface after baking (Fig. 4c and d).

Considering internal phase structure of PAcr/PB CPs film, it can be inferred that the protrusion was most probably resulted from the polysiloxane phase; meanwhile, the PB was also embedded in the polysiloxane phase. To confirm this inference, the compositions of the protrusion (red box) and flat substrate (blue box) of film were analysed by EDS. As shown in Fig. 5, it was found that the Si and Cu content of protrusion was much higher than that of flat substrate, giving additional support to above-mentioned conclusion.

Moreover, the effect of baking time on the film surface morphology and structure was examined by using AFM (Fig. 6). When the film was, some bulges were observed on the surface of film prepared at 25 °C (Fig. 6a). After baking for 0.5 min at 120 °C, the bulges disappeared to some degree (Fig. 6b). With the baking time increasing sequentially (1–5 min), more and more protrusions appeared and these protrusions became more obvious and spiculate (Fig. 6c–e). Just as shown in Fig. 6e, the roughness (R_a) of film increased gradually during the baking process.

Based on the FESEM, EDS and AFM results, these protrusions should be resulted from the phase separation of polysiloxane chain segments during baking. Generally, the interaction between acrylate polymers and the aluminum substrate is smaller than that between Si-containing groups and aluminium surface,[36] and it is easier for silicon-containing segments to erect on an aluminum surface than acrylate polymers. Moreover, during the annealing process, the silicon groups preferred to migrate to the air/polymer interface and occupy the outmost surface.[37,38]

Surface morphology of P(DMS-Acr)/PB film on printed fabric

The film formation process of P(DMS-Acr)/PB CPs on fabric surface was investigated in detail. As shown in Fig. 7a, original polyester fabric was made up of warp and weft yarns, and every yarn contained numerous filaments. It was evident that a lot of gaps existed between yarns, and the filaments were not adhered with each other. After coating with PAcr/PB CPs film and baking for 5 min, almost all of the gaps between yarns were covered by PAcr/PB CPs film (Fig. 7b). However, when ViPDMS content was kept at 10 wt% in P(DMS-Acr)/PB CPs film, some shrinkage holes were formed between yarns (Fig. 7c). With ViPDMS content increasing to 30 wt%, larger shrinkage holes were

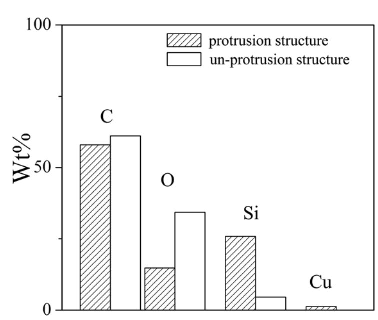

Fig. 5 Element distribution of protrusion and un-protrusion structure on the surface of PAcr/PB and P(DMS-Acr)/PB film.

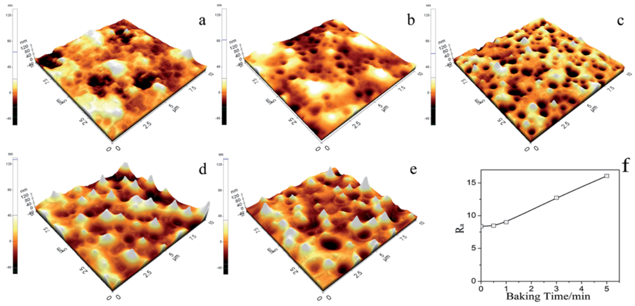

Fig. 6 AFM images of the composite film prepared by the P(DMS-Acr)/PB CPs at various baking times ((a) 0 min, (b) 0.5 min, (c) 1 min, (d) 3 min, (e) 5 min), (f) the effect of baking time on the R_a.

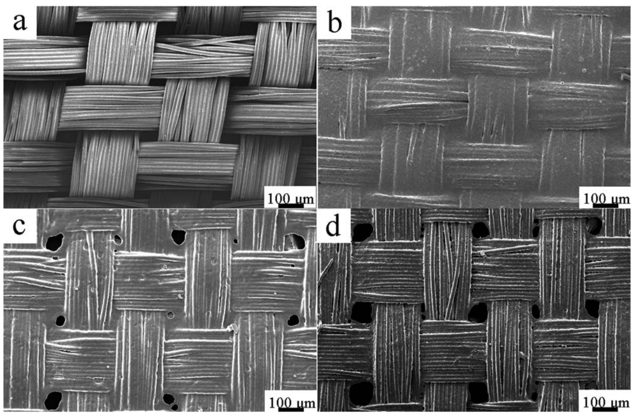

Fig. 7 Surface morphology of coated fabric with different ViPDMS content after baking 5 min ((a) uncoated fabric; (b) ViPDMS 10%; (c) ViPDMS 20%; (d) ViPDMS 30%).

observed (Fig. 7d). These results suggested that the P(DMS-Acr)/PB film would become discontinuous on the surface of the fabric after baking, especially when the ViPDMS content was high.

Moreover, the effect of ViPDMS content on surface microstructure of filaments was further examined (Fig. 8). In the absence of ViPDMS, the filaments were adhered with each other and the gaps between filaments were covered by the film (Fig. 8a). However, the gap between filaments became visible with increasing content of ViPDMS (Fig. 8b–d). It should be noted that the filaments were not adhered with each other when the ViPDMS content reached 30 wt%. Meanwhile, more and more protrusions were generated on filament surface with ViPDMS content increasing. Furthermore, the mean diameter of protrusions was estimated to be 0.72, 0.85 and 1.75 μm when ViPDMS content was kept at 10, 20 and 30 wt%, respectively (Fig. 9) and the water contact angle of the film increased from 76.5 to 103.7° because of the enrichment of hydrophobic polysiloxane segments on the surface. Those results were consistent with previous report that a higher ViPDMS content resulted in the formation of larger protrusions.[39]

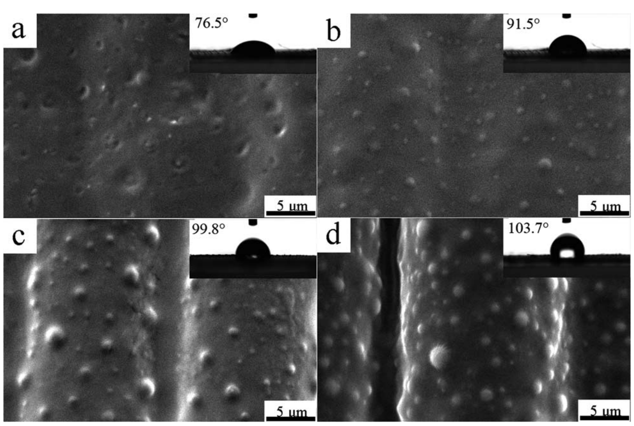

Fig. 8 Influence of ViPDMS content on the morphology of protrusion structure after baking 5 min, (a) 0%; (b) 10%; (c) 20; (d) 30%.

As mentioned above, when coated with P(DMS-Acr)/PB CPs emulsion, the polyester fabric could still retain majority of the gaps between yarns and between filaments after baking. Herein, the influence of baking time on the surface morphology and microstructure of printed fabric were further studied (Fig. 10). After coating with CPs emulsion at 25 °C, the gaps between filaments were covered by a continuous film, and only a small amount of tiny protrusions was observed on film surface (Fig. 10b). Nonetheless, a lot of protrusions appeared after baking at 120 °C for 1 min; moreover, the continuous film on filaments began to crack, and some gaps between filaments reappeared (Fig. 10c). After baking for 5 min, each filament was uniformly covered by the P(DMS-Acr)/PB CPs film and the protrusions on film surface became more marked; more importantly, majority of the gaps between filaments appeared again as compared with that before baking (Fig. 10d).

Based on above-mentioned film formation process, a film formation mechanism was proposed to interpret the microstructure evolution of P(DMS-Acr)/PB composite film on polyester fabric during baking (Fig. 11). As shown in Fig. 11, the surface of the fabric was covered by continuous P(DMS-Acr)/PB composite film before baking, and almost all of the gaps between the yarns were sealed by the composite film. However, after baking at 120 °C, the polysiloxane-containing polymers begin to flow quickly under gravitational field, due their low glass transition temperature and surface tension. As a result, the polymer filled in the gaps between yarns and between

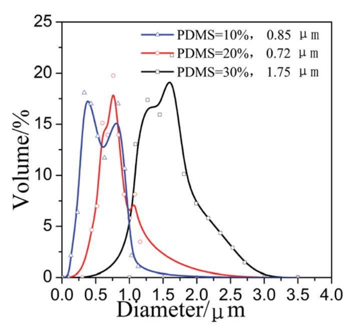

Fig. 9 The size distribution of protruding structures with various ViPDMS content (10%, 20%, 30%).

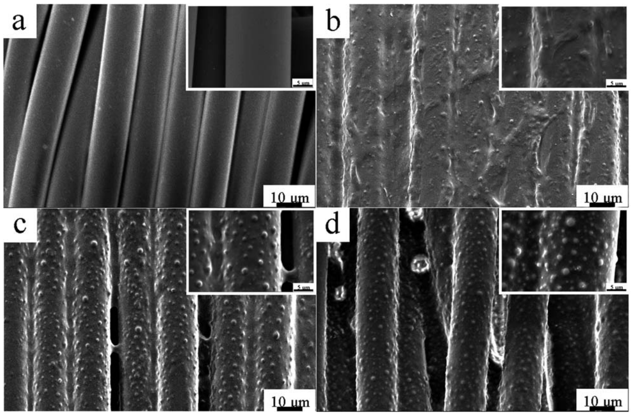

Fig. 10 Surface morphology of filament at different baking time ((a) uncoated; (b) baking 0 min; (c) baking 1 min; (d) baking 5 min).

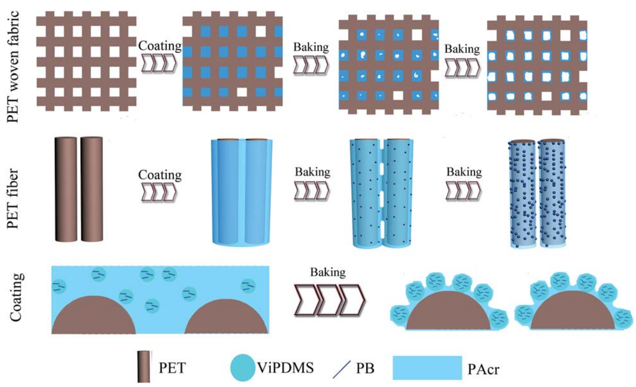

Fig. 11 Schematic representation of the film formation of the P(DMS-Acr)/PB CPs on the surface of different fabric structures during baking process.

filaments was consumed and successfully coated on every fiber, and hence majority of the gaps appeared again after baking. Meanwhile, phase separation occurred due to the incompatibility of polysiloxane and PAcr during baking and the PB particles preferred to distribute in polysiloxane island phase. Because of its lower surface energy, the polysiloxane component migrated to the film surface, and a lot of protrusions were eventually formed.

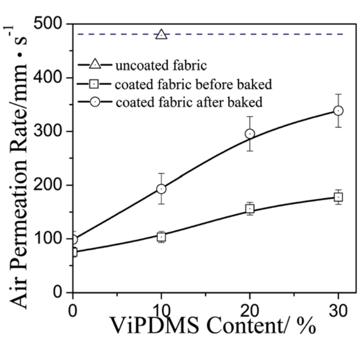

Fig. 12 Air permeability of printed fabric before and after baking.

Table 2 Rubbing fastness of the printed fabric

	Before baking		After baking	
Run	Dry	Wet	Dry	Wet
1	4	2	4	2–3
3	3–4	1–2	4	3
4	3–4	1–2	4–5	4
5	3	2	4–5	4–5

Performance of printed fabric

Printed fabric performances, such as air permeability, surface hydrophobicity, stiffness and rubbing fastness, are very important in practical application. Generally, it is difficult for conventional printing to balance the above-mentioned performances, especially for the breathability and rubbing fastness. The air permeability and relative stiffness of printed fabric was shown as Fig. 12. The air permeability of printed fabric was enhanced after baking, and increased from 100 to 350 mm s^{-1} with ViPDMS content increasing from 0 to 30 wt%.

The rubbing fastness refers to the degree of discoloration of printed fabrics after rubbing, which shows the adhesive strength of pigment and composite film on the surface of fabrics. The number of rubbing fastness is higher, the degree of adhesion was greater. As shown in Table 2, the rubbing fastness enhanced significantly after baking. Meanwhile, with increasing content of ViPDMS, more polysiloxane segment would migrate onto fabric surface, resulting in lower friction coefficient.[40,41] As a result, the rubbing fastness was also enhanced. When ViPDMS content increased from 0 to 30 wt%, the rubbing fastness of printed fabric raised at least two levels. All of these results indicated that the synthesized P(DMS-Acr)/PB composite was suitable and promising for fabric printing.

Conclusions

In this study, a series of P(DMS-Acr)/PB CPs were successfully synthesized *via* miniemulsion polymerization. Microstructure of the latex film was investigated in detail. It was found that phase separation occurred due to the incompatibility between polysiloxane and PAcr, and the PB particles mainly distributed in the polysiloxane island phase; meanwhile, a lot of protrusions were formed in the latex film after baking, and the protrusions became more obvious and spiculate with increasing amount of ViPDMS or baking time. When the P(DMS-Acr)/PB CPs were coated on the fabric, continuous film was formed at 25 °C, resulting in the coverage of the gaps between yarns and between fibers. However, during baking at 120 °C, the polymer could flow smoothly and be coated on the surface of every fiber; accordingly, the polymer filled in the gaps was consumed and the gaps appeared again; meanwhile, protrusions were also formed in this process because of lower surface energy of polysiloxane. Besides, the performance of the printed fabric was also evaluated. It was found that the printed fabric exhibited good air permeability, hydrophobicity, relative stiffness and rubbing fastness.

Conflicts of interest

There are no conflicts to declare.

Acknowledgements

This work was supported by National Natural Science Foundation of China (#U1609205); Zhejiang Sci-tech University Startup Research Fund (#18022114-Y)

References

1 M. Gsänger, D. Bialas, L. Z. Huang, M. Stolte and F. Würthner, *Adv. Mater.*, 2016, **28**, 3615–3645.
2 L. E. Hamilton and A. Chiweshe, *Starch/Staerke*, 1998, **50**(5), 213–218.
3 M. Li, L. P. Zhang, H. Y. Peng and S. H. Fu, *J. Appl. Polym. Sci.*, 2018, **135**(6), 45826–45835.
4 Y. Ding, M. Ye and A. J. Han, *J. Coating Technol. Res.*, 2018, **15**(2), 315–324.
5 P. P. Yin, G. Wu, W. L. Qin, X. Q. Chen, M. Wang and H. Z. Chen, *J. Mater. Chem. C*, 2013, **1**, 843–849.
6 Z. M. Hao and A. Iqbal, *Chem. Soc. Rev.*, 1997, **26**, 203–213.
7 M. Elgammal, R. Schneider and M. Gradzielski, *Dyes Pigments*, 2016, **133**, 467–478.
8 H. Najafi, M. E. Yazdanshenas and A. Rashidi, *Asian J. Chem.*, 2009, **21**(1), 433.
9 B. Neral, S. Šostar-Turk and B. Vončina, *Dyes Pigments*, 2006, **68**(2), 143–150.
10 M. M. El-Molla and R. Schneider, *Dyes Pigments*, 2006, **71**(2), 130–137.
11 S. H. Fu, L. Ding, C. Xu and C. Wang, *J. Appl. Polym. Sci.*, 2010, **117**(1), 211–215.
12 L. Hao, R. Wang, K. Fang and Y. Cai, *Ind. Crop. Prod.*, 2017, **95**, 348–356.
13 L. Hao, R. Wang, K. Fang, R. Liu and Y. Men, *Adv. Powder Technol.*, 2016, **27**(1), 164–170.
14 L. Wang, L. Zhang, Y. Zhang, M. Li and S. H. Fu, *Colloids Surf., A*, 2017, **533**, 33–40.
15 D. Nguyen, H. S. Zondanos, J. M. Farrugia, A. K. Serelis, C. H. Such and B. S. Hawkett, *Langmuir*, 2008, **24**(5), 2140–2150.
16 E. Bourgeat-Lami and M. Lansalot, *Hybrid latex particles*, Springer, Berlin, Heidelberg, 2010, pp. 53–123.
17 E. Bourgeat-Lami, E. A. França, T. C. Chaparro, R. D. Silva, P. Y. Dugas, G. M. Alves and A. M. Santos, *Macromolecules*, 2016, **49**(12), 4431–4440.
18 N. Steiert and K. Landfester, *Macromol. Mater. Eng.*, 2007, **292**(10–11), 1111–1125.
19 S. Gong, H. Chen, X. Zhou and S. Gunasekaran, *R. Soc. Open Sci.*, 2017, **4**(11), 170844.
20 O. A. Hakeim, H. A. Diab and J. Adams, *Prog. Org. Coating*, 2015, **84**, 70–78.
21 X. Fei, L. Cao and Y. Liu, *Dyes Pigments*, 2016, **125**, 192–200.
22 H. Widiyandari, F. Iskandar, N. Hagura and K. Okuyama, *J. Appl. Polym. Sci.*, 2008, **108**(2), 1288–1297.
23 H. Liu, S. Wen, J. Wang and Y. Zhu, *J. Appl. Polym. Sci.*, 2012, **123**(6), 3255–3260.
24 D. M. Qi, R. Zhang, L. Xu, Y. Yuan and L. Lei, *Acta Polym. Sin.*, 2011, **2**, 4–12.
25 A. Mese and K. G. Guzel, *J. Prosthet. Dent*, 2008, **99**(2), 153–159.
26 M. Zielecka and E. Bujnowska, *Prog. Org. Coating*, 2006, **55**(2), 160–167.
27 K. Huang, Y. Liu and D. Wu, *Prog. Org. Coating*, 2014, **77**(11), 1774–1779.
28 R. Bai, T. Qiu, M. M. Duan, G. Ma, L. He and X. Li, *Colloids Surf., A*, 2012, **396**, 251–257.
29 B. Pilch-Pitera, J. Kozakiewicz, I. Ofat, J. Trzaskowska and M. Špírková, *Prog. Org. Coating*, 2015, **78**, 429–436.
30 J. J. Kozakiewicz, I. Ofat, I. Legocka and J. Trzaskowska, *Prog. Org. Coating*, 2014, **77**(3), 568–578.
31 I. Marcu, E. S. Daniels, V. L. Dimonie, C. Hagiopol, J. E. Roberts and M. S. El-Aasser, *Macromolecules*, 2003, **36**(2), 328–332.
32 X. Jiang, J. Gu, X. Tian, D. Huang and Y. Yang, *J. Dispersion Sci. Technol.*, 2011, **32**(9), 1266–1272.
33 C. X. Huang, L. M. Yi and H. Y. Yuan, *Adv. Mater. Res.*, 2012, **441**, 478–483.
34 S. M. Shenava, A. B. Amin, R. M. Karant, S. J. Venkata and R. Ganugula, *Dyes Pigments*, 2016, **133**, 424–434.
35 Z. Cao, Q. Chen, H. N. Chen, Z. J. Chen, J. Yao, S. N. Zhao and D. M. Qi, *Colloids Surf., A*, 2017, **516**, 199–210.
36 D. Yu, Y. Zhao, H. Li, H. Qi, B. Li and X. Yuan, *Prog. Org. Coating*, 2013, **76**(10), 1435–1444.
37 S. Bas and M. D. Soucek, *J. Polym. Res.*, 2012, **19**(7), 9907.
38 M. Lin, F. Chu, A. Guyot, J. L. Putaux and E. Bourgeat-Lami, *Polymer*, 2005, **46**(4), 1331–1337.
39 J. Khanjani, S. Pazokifard and M. J. Zohuriaan-Mehr, *Prog. Org. Coating*, 2017, **102**, 151–166.
40 Q. Zhang and M. H. Wu, *J. Appl. Polym. Sci.*, 2019, 47961–47968.
41 L. Wang, S. Cui, H. Ni, M. H. Wu and W. Wang, *Prog. Org. Coating*, 2018, **123**, 75–81.